Reversal of a Mutator Activity by a Nearby Fidelity-Neutral Substitution in the RB69 DNA Polymerase Binding Pocket

ARTICLE *in* JOURNAL OF MOLECULAR BIOLOGY · OCTOBER 2010

Impact Factor: 4.33 · DOI: 10.1016/j.jmb.2010.09.058 · Source: PubMed

5 AUTHORS, INCLUDING:

Anna Trzemecka
Polish Academy of Sciences
6 PUBLICATIONS **20** CITATIONS
SEE PROFILE

Anna Bebenek
Polish Academy of Sciences
12 PUBLICATIONS **583** CITATIONS
SEE PROFILE

doi:10.1016/j.jmb.2010.09.058 J. Mol. Biol. (2010) 404, 778–793

Contents lists available at www.sciencedirect.com

Journal of Molecular Biology

journal homepage: http://ees.elsevier.com.jmb

Reversal of a Mutator Activity by a Nearby Fidelity-Neutral Substitution in the RB69 DNA Polymerase Binding Pocket

Anna Trzemecka[1], Agata Jacewicz[1], Geraldine T. Carver[2], John W. Drake[2] and Anna Bebenek[1]*

[1]*Department of Molecular Biology, Institute of Biochemistry and Biophysics, Polish Academy of Sciences, Pawinskiego 5a, 02-104 Warsaw, Poland*
[2]*Laboratory of Molecular Genetics, National Institute of Environmental Health Sciences, Research Triangle Park, NC 27709, USA*

Received 29 July 2010; received in revised form 27 September 2010; accepted 28 September 2010
Available online 13 October 2010

Edited by M. Gottesman

Keywords:
Exo;
Pol

Phage RB69 B-family DNA polymerase is responsible for the overall high fidelity of RB69 DNA synthesis. Fidelity is compromised when conserved Tyr567, one of the residues that form the nascent polymerase base-pair binding pocket, is replaced by alanine. The Y567A mutator mutant has an enlarged binding pocket and can incorporate and extend mispairs efficiently. Ser565 is a nearby conserved residue that also contributes to the binding pocket, but a S565G replacement has only a small impact on DNA replication fidelity. When Y567A and S565G replacements were combined, mutator activity was strongly decreased compared to that with Y567A replacement alone. Analyses conducted both *in vivo* and *in vitro* revealed that, compared to Y567A replacement alone, the double mutant mainly reduced base substitution mutations and, to a lesser extent, frameshift mutations. The decrease in mutation rates was not due to increased exonuclease activity. Based on measurements of DNA binding affinity, mismatch insertion, and mismatch extension, we propose that the recovered fidelity of the double mutant may result, in part, from an increased dissociation of the enzyme from DNA, followed by the binding of the same or another polymerase molecule in either exonuclease mode or polymerase mode. An additional antimutagenic factor may be a structural alteration in the polymerase binding pocket described in this article.

Introduction

The DNA polymerases (gp43 s encoded by gene *43*) of the related bacteriophages T4 and RB69 synthesize DNA with high fidelity, inserting one wrong nucleotide per 10^5 replicated bases.[1] These polymerases belong to the B-family—the same family that is populated by the eukaryotic replicative polymerases α, δ, and ε. For RB69 DNA polymerase, crystal structures are available for the apo enzyme,[2] a binary editing complex with DNA bound in the exonuclease domain,[3] and ternary complexes (replicating complex) with DNA and dNTP bound in the polymerase site.[4] Because of the availability of crystal structures in so many conformations, RB69 polymerase is a good structural model for studying the mechanisms responsible for high base selectivity.

RB69 DNA polymerase achieves its fidelity by the coordinated action of two activities: a polymerase (Pol) activity that is responsible for correct

*Corresponding author. E-mail address: aniab@ibb.waw.pl

Abbreviations used: dsDNA, double-stranded DNA; ssDNA, single-stranded DNA.

nucleotide selection and an exonuclease (Exo) activity that removes mismatched nucleotides from the primer terminus. As with all polymerases that replicate DNA with high fidelity, binding the correct incoming dNTP introduces conformational changes in both the enzyme and the DNA. The fingers subdomain undergoes the largest conformational change, moving toward the palm subdomain to enclose the incoming dNTP and the complementary template nucleotide and thus to generate a binding pocket for the nascent base pair.[4–7]

In the RB69 polymerase, the active Pol binding site is formed by several highly conserved residues located in the fingers and palm. Arg482 and Lys560 in the fingers are involved in hydrogen bonding to the phosphate groups of the incoming dNTP. Hydrophobic interactions with the nascent base pair are formed by Leu415 and Tyr416 on the minor groove side and by Tyr567 and Gly568 on the template side. Asn564 and Ser565 form the rear wall of the binding pocket and ensure a coplanar base arrangement of the nascent base pair (M. Wang *et al*., unpublished results).[1,4,8]

All of these residues play important roles in RB69 DNA replication fidelity. Leu415 and Tyr567 are critical for substrate discrimination. L415F/G mutants have elevated rates for a variety of base substitution errors and single-base deletions in repetitive and nonrepetitive sequences.[8] Replacing Tyr567 by Ala, Ser, or Thr confers a strong mutator phenotype, particularly for base substitution errors.[1] Tyr416 is responsible for discriminating between ribose moiety and deoxyribose moiety in incoming nucleotides,[9] while Leu561 discriminates sterically against mismatches in the nascent base-pair binding pocket.[10] Thus, the size and shape of the polymerase binding pocket play crucial roles in replication fidelity.

Insertion of a wrong nucleotide compromises the rate of primer extension. The polymerase stalls, altering the balance between extension by the polymerase and excision by the mismatch-editing exonuclease. Newly incorporated mismatches reduce the efficiency of subsequent nucleotide insertions and extensions by 10^2-fold to 10^6-fold,[6,7,11,12] with the magnitude depending on the mismatch and the polymerase.

Polymerases with compromised fidelity due to alterations at the Pol site may display reduced partitioning to the Exo site and thus favor mismatch extension over proofreading, notably with the T4 Pol^{L412M} and RB69 $Pol^{L415F/G}$ mutants.[8,13] The same mechanism probably applies to the RB69 Pol^{Y567A} mutant, as previously proposed.[1] Conversely, T4 polymerase mutants (such as $T4^{A737V}$) that display an antimutator phenotype, mainly reducing A·T → G·C rates, tend to display a decreased ability to translocate after nucleotide incorporation, thus favoring the formation of exonuclease complexes and increasing the efficacy of proofreading.[14,15] In preliminary screens, we observed that the RB69 S565G replacement had only weak impacts on fidelity; however, surprisingly, when the Y567A and S565G replacements were combined within the highly conserved B-motif $KX_3N\mathbf{S}X\mathbf{Y}G$, the powerful mutator activity of the Pol^{Y567A} mutation was strongly reduced. To better understand the role of Ser565 in fidelity, we characterized some of the biochemical properties of RB69 polymerase mutants containing S565G replacement, Y567A replacement, or both replacements. We also investigated the impact of these replacements using fidelity assays both *in vivo* and *in vitro*. Our results led us to propose that introducing the S565G replacement lowers the DNA binding affinity of the polymerase and increases its ability to dissociate from the primer/template, thus increasing the opportunity for proofreading by the same or another polymerase molecule (proofreading in trans) and contributing to the antimutagenic impact of S565G on Y567A.

Results

Bacteriophage RB69 gp43 Y567 and S565 are highly conserved residues within the B-family of DNA polymerases and are located in the region involved in dNTP binding. We showed previously that Y567 plays a crucial role in base selection: when Y567 was replaced with A, S, or T, the mutant polymerase displayed severely decreased fidelities both *in vivo* and *in vitro*.[1] To study the role of S565, we replaced it with G in both Exo^+ and Exo^- backgrounds. We also examined the combinatorial effect of the double replacement Y567A/S565G. Most of the assays were performed using Exo^+ derivatives because of the surprising antimutator effect of the double replacement in this background.

Polymerase activity *in vivo* and specific activity *in vitro*

In assays *in vivo*, we often used a hybrid system in which T4, whose own gp43 is inactivated by amber mutations at codons 202 and 386 (T4 *43amam*), is replicated by wild-type or mutant RB69 gp43 s expressed from plasmids.[1] Polymerase activity *in vivo* was determined only for Exo^+ derivatives. DNA synthesis by T4 gp43 was totally blocked by a *43amam* mutation and performed instead by one of the RB69 DNA polymerases expressed from a plasmid. DNA synthesis was measured in infected *Escherichia coli* cells at a time when host DNA synthesis had ceased completely.[1] DNA synthesis was moderate in the presence of S565G either alone (30% of wild-type activity) or in combination with Y567A (40% of wild-type activity), while the Y567A mutant retained 50% activity.

Table 1. Mutation rates for RB69 Exo$^+$ DNA polymerase mutants in *rII* reversion assays

*rII*tester mutation tester mutation	Mutation scored	Reversion rate × 10^8			
		Pol$^+$ [17]	Pol^{S565G} [6–7]	Pol^{Y567A} [7]	Pol$^{S565G/Y567A}$ [13–14]
131	+1	9.0 (1)	4.3 (0.5)	37 (4.0)	5.6 (0.6)
UV232	−1	1.0 (1)	3.3 (3.3)	210 (210)	4.4 (4.5)
UV256	G·C→A·T	6.4 (1)	15 (2.4)	7200 (1100)	130 (20)
UV375	A·T→any	1.6 (1)	0.5 (0.3)	2600 (1700)	28 (18)

Values in brackets are the numbers of stocks providing the median rate. Values in parentheses below each rate are relative to those for Pol$^+$. The entries for Pol$^+$ and Pol^{Y567A} were adapted from a previous article.[1]

We also measured polymerase-specific activity *in vitro* for the RB69 DNA polymerases using activated DNA as substrate. The specific activities for the Exo$^+$ versions of Pol^{Y567A}, Pol$^{Y567A/S565G}$, and Pol^{S565G} were 80%, 72%, and 47%, respectively, of the Pol$^+$ Exo$^+$ value.

Fidelity *in vivo*

In *rII* reversion assays (Table 1), RB69 Pol^{S565G} has almost negligible impact on replication fidelity for both base substitutions and frameshifts; the average change in mutation rates was a 2-fold increase compared to the wild-type enzyme. Similarly, in *rI* forward mutation assays (Table 2), Pol^{S565G} in Exo$^+$ background had a mutation rate elevated by a factor of 5 compared to the wild-type enzyme; in Exo$^-$ background, no significant difference (rate decreased 0.8-fold) was observed between parental enzymes and mutant enzymes. Surprisingly, the double mutant (Pol$^{S565G/Y567A}$ Exo$^+$) had strongly decreased mutator activities compared to the Pol^{Y567A} Exo$^+$ mutant in *rII* reversion assays: the second replacement (at S565) suppressed most of the mutator traits of the Y567A replacement. The most striking results were the 90-fold decrease in base substitution mutation rates at the *UV375* A·T site and the 60-fold decrease in base substitution mutation rates at the *UV256* G·C→A·T site, while −1 and +1 frameshift mutations were reduced by 50-fold and 6-fold, respectively, at other sites (Table 1). In *rI* forward mutation assays, the Pol$^{S565G/Y567A}$ double mutant decreased mutation rates by 40-fold compared to the single Pol^{Y567A} mutant (Table 2). In Exo$^-$ background, the Pol$^{S565G/Y567A}$ mutant did not support the production of viable T4 *43amam* progeny, perhaps because of a lethally high mutation rate from the combination of the mutator effects of the Y567A replacement and the Exo deficiency[1,16]—a combination that the S565G mutation may reduce insufficiently to restore viability.

We sequenced independent *rI* mutants from experiments in which T4 *43amam* phage was replicated by the RB69 polymerase mutants Pol^{S565G} Exo$^+$ and Pol$^{S565G/Y567A}$ Exo$^+$, respectively. The kinds of mutations made by these polymerases are shown in Table 3, together with the kinds obtained previously for the Pol$^+$ and Pol^{Y567A} enzymes.[1,16] Mutations produced by the Pol^{S565G} Exo$^+$ polymerase were very similar to those produced by the Pol$^+$ Exo$^+$ polymerase; the complex mutations were almost all GCG→CTA at the 146–148 hot spot.[16–18] There were no strong differences between the kinds of mutations produced by Pol$^{S565G/Y567A}$ Exo$^+$ polymerases and the kinds of mutations produced by Pol^{Y567A} Exo$^+$ polymerases, each making predominantly base substitutions. G→A predominated among transition mutations, with as much as 70% localized at a hot spot at *rI* base 247. C→T and C→A mutations at another hot spot at *rI* base 202 were also present in the spectra produced by both

Table 2. Forward mutation rates of RB69 DNA polymerase mutants *in vivo*

Polymerase	Number of stocks	Mutation rate × 10^5	Relative rate
Pol$^+$ Exo$^+$	7	0.43	1
Pol^{S565G} Exo$^+$	7	2.1	5
Pol^{Y567A} Exo$^+$	7	210	490
Pol$^{S565G/Y567A}$ Exo$^+$	11	5.5	13
Pol$^+$ Exo$^-$	7	220	510
Pol^{S565G} Exo$^-$	7	180	430

The entries for Pol$^+$ Exo$^+$, Pol$^+$ Exo$^-$, and Pol^{Y567A} Exo$^+$ were adapted from previous articles.[1,14]

Table 3. Classes of *rI* mutations generated by Exo$^+$ RB69 DNA polymerase mutants

	Polymerase			
	Pol$^+$	Pol^{S565G}	Pol^{Y567A}	Pol$^{S565G/Y567A}$
Number of mutations	103	53	79	45
A·T→G·C	7	0	25	5
G·C→A·T	22	6	43	27
Transitions	29	6	68	32
A·T→T·A	0	2	0	0
A·T→C·G	2	0	2	3
G·C→T·A	34	22	8	7
Transversions	36	24	10	10
±1	10	6	1	2
≥±2	7	2	0	0
Complex	21	15	0	1
GCG→CTA				

The Pol$^+$ and Pol^{Y567A} entries were adapted from previous articles.[1,17]

Fig. 1. *rI* mutational spectra for the RB69 Pol $^{S565G/Y567A}$ Exo$^+$ and Pol^{Y567A} Exo$^+$ polymerases. The sequence represents the wild-type *rI* strand complementary to the coding strand, with every 10th base in boldface. Upper-case letters indicate base substitutions. The addition of a single base is indicated by "+." The underlined three-base mutation at residues 146–148 is a hot spot for complex mutations. The entries for Pol^{Y567A} were adapted from a previous article.[1]

Pol^{Y567A} Exo$^+$ and Pol$^{S565G/Y567A}$ Exo$^+$ polymerases (Fig. 1). Only A→G mutations were underrepresented in this spectrum, with only one appearing, while 11 were found in the Pol^{Y567A} Exo$^+$ spectrum (Table 3). Thus, the decreased mutation rates in the double mutant hardly affected specificity but merely lowered the overall mutation rate.

Fidelity *in vitro*

To learn more about the role of Ser565 in fidelity, we conducted studies *in vitro* using the *lacZ*α DNA template in gapped M13mp2 DNA (Table 4). The *lacZ*α mutant frequencies for the Pol$^+$ Exo$^+$ and Pol^{S565G} Exo$^+$ mutants were 8×10^{-4} and 4×10^{-4}, respectively, with the values indistinguishable from each other, similar to the 5×10^{-4} to 7×10^{-4} frequencies typically obtained with gapped DNA,[16,19] and representing only the mutations that accumulated during the growth of the M13 phage stock. The *lacZ*α mutant frequency for the Pol^{Y567A} Exo$^+$ mutant in earlier studies was 55×10^{-4}, and we observed a 5-fold decrease in mutation frequency when the DNA was copied by the Pol$^{S565G/Y567A}$ Exo$^+$ polymerase. This frequency (10×10^{-4}) was close to that of the Pol$^+$ Exo$^+$ polymerase. These results were fully consistent with those obtained in our fidelity studies conducted *in vivo*.

The *lacZ*α mutant frequency for the Pol^{S565G} Exo$^-$ polymerase was 14×10^{-4}, modestly lower that the 29×10^{-4} frequency obtained previously with the Pol$^+$ Exo$^-$ enzyme. The Pol$^{S565G/Y567A}$ Exo$^-$ polymerase was more proficient in proofreading some errors than was the Pol^{Y567A} Exo$^-$ polymerase (Table 4; 89×10^{-4} *versus* 164×10^{-4}). However, the Pol$^{S565G/Y567A}$ Exo$^-$ polymerase retained a high mutation frequency, which probably resulted in lethally mutated progeny during growth *in vivo*.

Table 4. Fidelities of RB69 polymerases in *lacZ*α forward mutation tests *in vitro*

Pol	Exo	MF × 10^4	Mutations	Base substitutions	−1	Other
Pol$^+$	+	8.4	22	20	2	—
Pol^{S565G}	+	3.6	—	—	—	—
Pol^{Y567A}	+	55	147	110	37	—
Pol$^{S565G/Y567A}$	+	10.4	100	55	31	14
Pol$^+$	–	29	159	93	40	26
Pol^{S565G}	–	14	48	24	15	9
Pol^{Y567A}	–	164	154	120	28	6
Pol$^{S565G/Y567A}$	–	89	103	75	25	3

MF, mutation frequency. Mutations are numbers detected by sequencing; mutants from the Pol^{S565G} Exo$^+$ polymerase were not sequenced because the mutant frequency was at the historical background for uncopied DNA. "Other" mutations consisted of larger deletions and a few complex mutations.
The data for Pol$^+$ and Pol^{Y567A} were adapted from a previous article.[17]

The contribution of S565G to the fidelity of Pol$^{S565G/Y567A}$

As previously reported,[16] the RB69 Pol^{Y567A} Exo$^+$ polymerase is a strong base substitution mutator *in vitro*, mostly for transition mutations (especially for T→C produced by T·G mispairs) but also for frameshift mutations in homopolymeric runs, while frameshift mutations in runs were almost absent *in vivo*. The Pol$^{S565G/Y567A}$ Exo$^+$ double mutant also produced base substitutions, again

Table 5. RB69 DNA polymerase mutation specificities in *lacZα* forward mutation tests *in vitro*

	Pol^{Y567A} Exo^+		$Pol^{S565G/Y567A}$ Exo^+		Pol^+ Exo^-		Pol^{S565G} Exo^-		Pol^{Y567A} Exo^-		$Pol^{S565G/Y567A}$ Exo^-	
	147		100		159		48		154		103	
Mutations	*n*	μ	*n*	μ	*n*	μ	*n*	μ	*n*	μ	*n*	μ
Base substitutions	110	47	55	3.4	93	17	24	4.4	120	160	75	78
A→G (A·dCMP)	2	6	3	1.3	1	1	2	2.5	0	≤9	7	≤7
G→A (G·dTMP)	7	18	6	2.2	8	9	2	2.1	54	420	20	122
C→T (C·dAMP)	17	38	17	5.4	45	42	9	8.5	12	82	1	37
T→C (T·dGMP)	76	150	15	4.3	13	11	4	3.4	37	230	33	158
Transitions	102	60	41	3.5	67	17	17	4.3	103	187	61	85
A→C (A·dGMP)	0	≤3	2	0.9	1	1	0	≤1.4	1	10	1	8
A→T (A·dAMP)	2	5	0	≤0.35	1	1	1	1.2	2	15	2	12
T→G (T·dCMP)	0	≤2	0	≤0.35	0	≤1	0	≤1	0	≤7	5	29
T→A (T·dTMP)	2	7	5	2.5	0	≤1	0	≤1.5	8	85	4	33
G→T (G·dAMP)	1	2	4	1.3	15	14	4	3.8	2	14	1	5
G→C (G·dGMP)	2	6	2	0.8	7	8	1	1.2	4	34	1	6
C→A (C·dTMP)	1	3	1	0.47	1	1	0	≤1.4	0	≤10	1	7
C→G (C·dCMP)	0	≤5.8	0	≤0.9	1	3	1	2.6	0	≤19	0	≤15
Transversions	8	2.9	14	0.7	26	4.1	7	1.1	17	19	15	13
±1	37	10	31	1.3	40	5	15	1.8	28	24	25	17
–(residues 2–436)	0	≤55	12	96	23	540	8	189	5	850	3	401
Other	0	≤55	2	16	3	71	1	27	1	170	0	≤134

Mutation rates (μ) are incorporated per 10^6 nucleotides. "≤" values were calculated as if one mutant had been detected. Mutation rates for the Pol^+ Exo^+ and Pol^{S565G} Exo^+ polymerases are not displayed because of the lack of signals significantly above the historical background. Values for Pol^{Y567A} Exo^+, Pol^+ Exo^-, and Pol^{Y567A} Exo^- were adapted from a previous article.[16] The number of detectable sites is not defined for deletions >1 nt, and their mutation rates are therefore not normalized to the number of opportunities and thus only appear to be larger than other normalized values.

mostly transition mutations. This polymerase also produced frameshift mutations and large deletions not seen in the Pol^{Y567A} Exo^+ spectrum (Table 5). Among 12 large deletions, 11 (of 27–371 nucleotides) occurred between direct repeats. Most of the frameshift mutations occurred at runs of two or more repeated bases.

The roster of mutational classes showed a significant decrease in T→C transitions with the double replacement compared to that with Pol^{Y567A} alone. There were at least five sequence contexts where T→C mutations either were absent or appeared only once in the double-mutant spectrum but were strongly represented in the single-mutant spectrum (Fig. 2a). Overall, base substitution rates decreased by 14-fold in the double mutant, with the decrease in T·dGMP rates being as much as 35-fold compared to the Pol^{Y567A} polymerase (Table 5). The other transition mutation rates decreased 7-fold for C·dATP, 8-fold for G·dTMP, and 5-fold for A·dCMP. Transversion mutations were less frequent in the spectra of both polymerases. A·dAMP rates decreased 14-fold, G·dGMP rates decreased 7-fold, and C·dTMP rates decreased 6-fold; for the remaining mismatches, the mutation rates decreased 3-fold to 1.5-fold (Table 5). Frameshift mutation rates decreased about 8-fold in the double mutant compared to the single mutant.

We did not sequence *lacZα* mutants from the Pol^{S565G} Exo^+ polymerase background because the mutation frequency (4×10^{-4}) for this polymerase was at the level of the historical background frequency (5.7×10^{-4} to 6.2×10^{-4}) for unfilled template DNA. This low mutation frequency probably recorded the intrinsic mutation frequency resulting from phage M13 replication and made further analysis of the Pol^{S565G} Exo^+ polymerase unreliable.

The contribution of proofreading to the fidelity of the $Pol^{S565G/Y567A}$ Exo^+ polymerase

The *lacZα* mutation frequency for the $Pol^{S565G/Y567A}$ Exo^- polymerase (89×10^{-4}) was 6-fold higher that that for the Pol^{S565G} Exo^- polymerase (14×10^{-4}) and about 2-fold lower than that for the Pol^{Y567A} Exo^- mutant (164×10^{-4}). The $Pol^{S565G/Y567A}$ Exo^- polymerase had reduced nucleotide selectivity compared with the parental Pol^+ Exo^- polymerase, but was less error prone than the Pol^{Y567A} Exo^- polymerase. Proofreading improved fidelity 8-fold in the $Pol^{S565G/Y567A}$ Exo^+ polymerase but only 3-fold in the Pol^{Y567A} Exo^+ polymerase (Table 4). Proofreading in the $Pol^{S565G/Y567A}$ double mutant removed both base mismatches and frameshift mutations. The error rates for all 12 possible base mismatches over all detectable sites in the *lacZα* template and for Exo^+ and Exo^- single and double Pol mutants are presented in Table 5. In Exo^- background, the spectra for the single and double mutants showed no striking differences, and the distribution of mutations along the *lacZα* sequence revealed no significant differences between the two enzymes (Fig. 2b and c).

Exonuclease activities of single and double Pol mutants

One possible explanation for the observed decrease in mutation rates in the Pol$^{S565G/Y567A}$ mutant would be increased exonuclease activity. We therefore conducted exonuclease assays on substrates with either a correct base pair or a T·dGMP mismatch at the 3′ terminus to compare the various polymerase variants. However, both Pol^{S565G} and Pol$^{S565G/Y567A}$ polymerases were less efficient than the wild-type and Pol^{Y567A} polymerases in

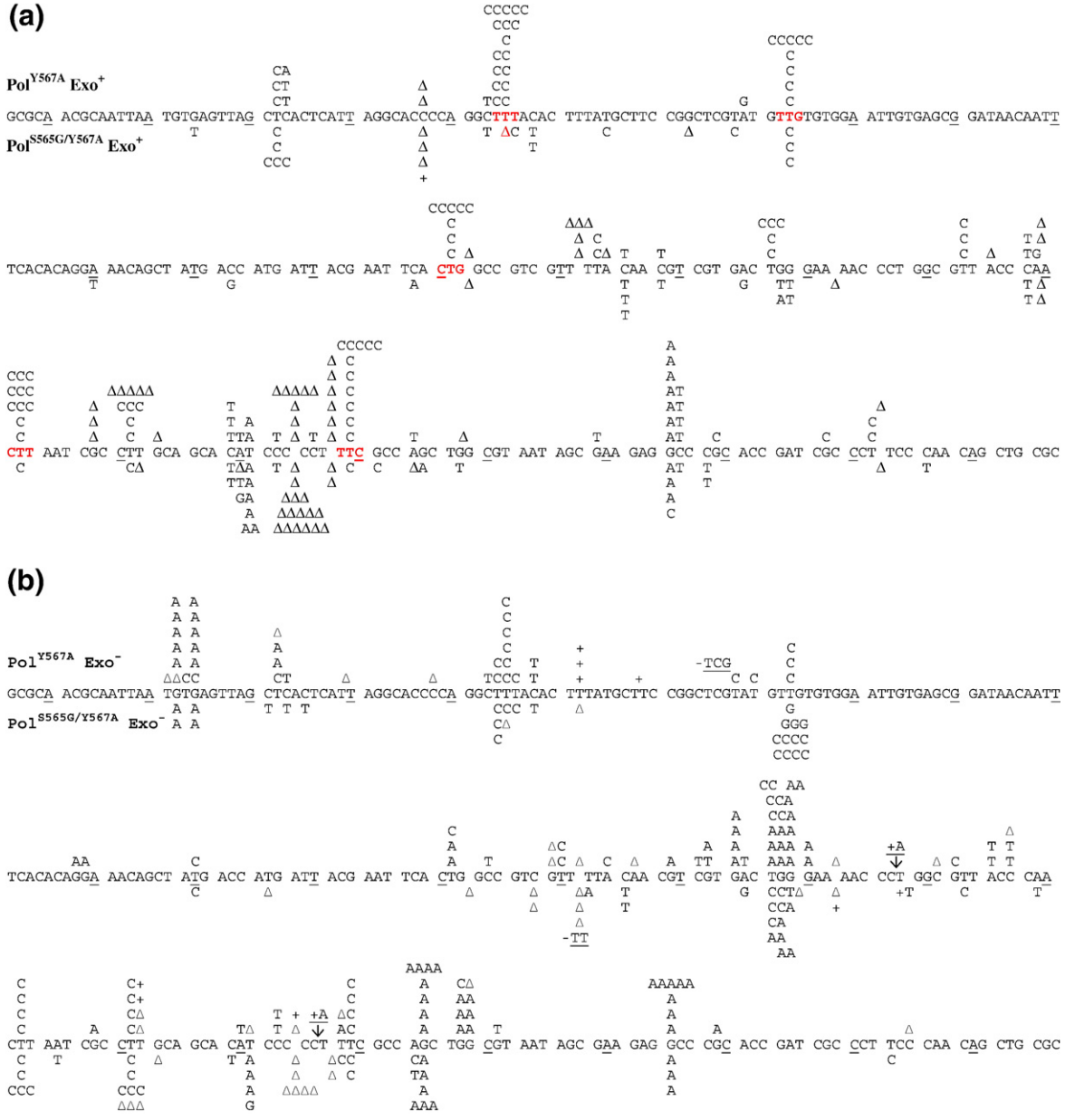

Fig. 2. *lacZ*α mutational spectra. The 5′→3′ sequence of the viral template strand of the *lacZ*α sequence in M13mp2 is shown from position −84 through position +197, where +1 is the first transcribed base and every 10th base is underlined. Upper-case letters indicate base substitutions. The deletion of a single base is indicated by "Δ," whereas the addition of a single base is indicated by "+." Large deletions and complex mutations are not shown. (a) Spectra for Pol^{Y567A} Exo$^+$ (above the *lacZ*α sequence) and Pol$^{S565G/Y567A}$ Exo$^+$ (below the *lacZ*α sequence). The five *lacZ*α base triplets in red are positions where significant differences were observed between the two spectra. (b) Spectra for Pol^{Y567A} Exo$^-$ (above) and Pol$^{S565G/Y567A}$ Exo$^-$ (below). (c) Spectra for Pol$^{S565G/567A}$ Exo$^+$ (above) and Pol$^{S565G/Y567A}$ Exo$^-$ (below). The spectra for Pol^{Y567A} were adapted from a previous article.[17]

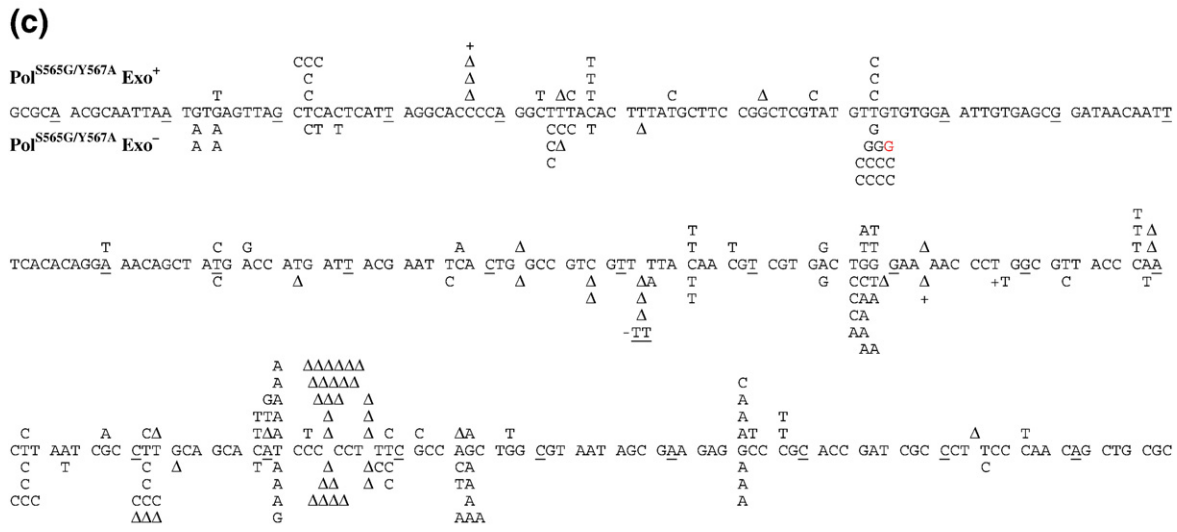

Fig. 2 (*continued*)

degrading double-stranded DNA (dsDNA) with either a correct primer terminus base pair or an incorrect primer terminus base pair (Fig. 3a and b). The exonuclease activity on single-stranded DNA (ssDNA) was indistinguishable among the Pol^{+}, Pol^{Y567A}, and Pol$^{S565G/Y567A}$ polymerases, but was slightly reduced in the Pol^{S565G} polymerase (Fig. 3c).

DNA binding activity

Decreased exonuclease activity may result from a change in the dynamic equilibrium between the formation of complexes at the Pol active site and the formation of complexes at the Exo active site.[13] A mismatch at the 3′ terminus usually increases Exo activity by weakening Pol binding to the substrate.[7] Using gel retardation assays, we measured the strength of dsDNA binding for Pol^{+}, Pol^{Y567A}, Pol^{S565G}, and Pol$^{S565G/Y567A}$ polymerases in Exo^{+} backgrounds with either a normal terminal base pair or a terminal T·dGMP mismatch using the same substrates as for the exonuclease assays (Fig. 4a and b). $K_{d(DNA)}$ values were then determined from reciprocal plots of enzyme concentration (Table 6). The Pol^{S565G} polymerase had the highest dissociation constants when binding correctly paired DNA ($K_{d(DNA)}$ = 38.9 nM) or the mismatched substrate ($K_{d(DNA)}$ = 132 nM). These dissociation constants were about 6-fold higher than for the Pol^{+} polymerase and 3-fold higher than for the Pol^{Y567A} polymerase on normal dsDNA, and 3-fold higher for the Pol^{+} polymerase and 5-fold higher for the Pol^{Y567A} polymerase on dsDNA with the mismatch. The Pol$^{S565G/Y567A}$ polymerase also bound less strongly to both substrates compared to the Pol^{+} and Pol^{Y567A} polymerases ($K_{d(DNA)}$ = 29.9 nM for normal dsDNA and $K_{d(DNA)}$ = 79.9 nM for mismatched dsDNA, compared with $K_{d(DNA)}$ = 6.9 nM and $K_{d(DNA)}$ = 13.2 nM for Pol^{+} and Pol^{Y567A} polymerases on correctly paired dsDNA, and $K_{d(DNA)}$ = 38.2 nM and $K_{d(DNA)}$ = 25.7 nM for Pol^{+} and Pol^{Y567A} polymerases on mismatched dsDNA, respectively).

Weaker DNA binding in the Pol site does not correlate with decreased dsDNA exonuclease activity for the Pol^{S565G} or Pol$^{S565G/Y567A}$ polymerase. Thus, both enzymes probably dissociate from either normal or mismatched primer/template substrates more often that do either the Pol^{+} polymerase or the Pol^{Y567A} polymerase.

Primer-extension activities

The error rate of the Pol$^{S565G/Y567A}$ Exo^{+} polymerase is decreased for almost all mispairs compared to the Pol^{Y567A} Exo^{+} polymerase. These differences are also observed in Exo^{-} background and thus may not simply reflect partitioning ratios between the Pol sites and the Exo sites. Analysis of mutation spectra for the Pol$^{S565G/Y567A}$ Exo^{+} and Pol^{Y567A} Exo^{+} polymerases showed that, among transition mutations, the biggest difference was in extending T·dGMP mismatches (Table 5). Therefore, we used standing-start and running-start assays to measure the abilities of the Pol^{+}, Pol^{Y567A}, and Pol$^{S565G/Y567A}$ polymerases (all in Exo^{+} backgrounds) to insert dGTP opposite T and to extend the T·dGMP mismatch.

The Pol^{+} and Pol^{S565G} polymerases misinsert dGTP inefficiently opposite a template T (Fig. 5) and also extend a T·dGMP mismatch inefficiently (Fig. 6). The Pol^{Y567A} polymerase both generates and extends T·dGMP mismatches more efficiently (Figs. 5 and 6). The Pol$^{S565G/Y567A}$ polymerase is

much less efficient in both insertion and extension (Figs. 5 and 6). The same pattern was observed in running-start assays: the Pol^{+} and Pol^{S565G} polymerases were unable to detectably insert dGTP opposite template T. The Pol^{Y567A} polymerase both inserted and extended a mismatch, while the $Pol^{S565G/Y567A}$ polymerase was again much less efficient in both steps (Fig. 7). The Exo^{-} variants of the Pol^{+}, Pol^{S565G}, and $Pol^{S565G/Y567A}$ polymerases were similarly less efficient in both activities, in contrast to the Pol^{Y567A} polymerase, which inserted and extended the T·dGMP mismatch efficiently (data not shown).

The $Pol^{S565G/Y567A}$ Exo^{-} polymerase supports the replication of T4 phage *in vivo*

It was reported previously that the Pol^{Y567A} Exo^{-} polymerase was unable to support the *in vivo* growth of either T4 *43amam* or T4 43^{+1}. This dominant-lethal phenotype was ascribed to the low fidelity of DNA synthesis conducted by this enzyme, resulting in

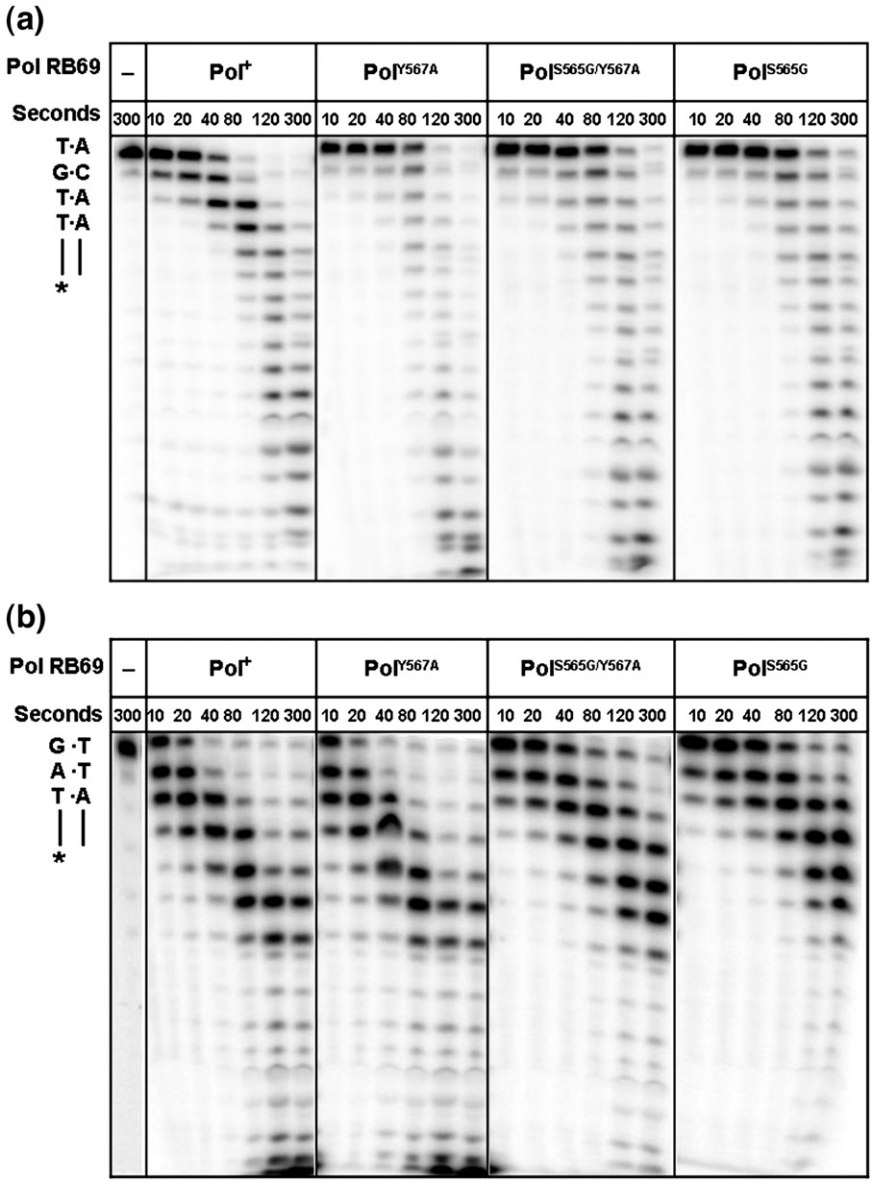

Fig. 3. Exonuclease activities of RB69 DNA polymerases on ssDNA using a ^{32}P-labeled 20-mer, on normal dsDNA using a ^{32}P-labeled 20-mer/35-mer, and on dsDNA containing a terminal G·T mismatch using a ^{32}P-labeled 20-mer/35-mer. Reactions were incubated at 37 °C for 10 s, 20 s, 40 s, 80 s, and 300 s. Products of degradation were analyzed by electrophoresis on a 15% polyacrylamide gel with 7 M urea, followed by autoradiography. Exonuclease assays on (a) normal dsDNA, (b) dsDNA with a terminal G·T mismatch, and (c) ssDNA.

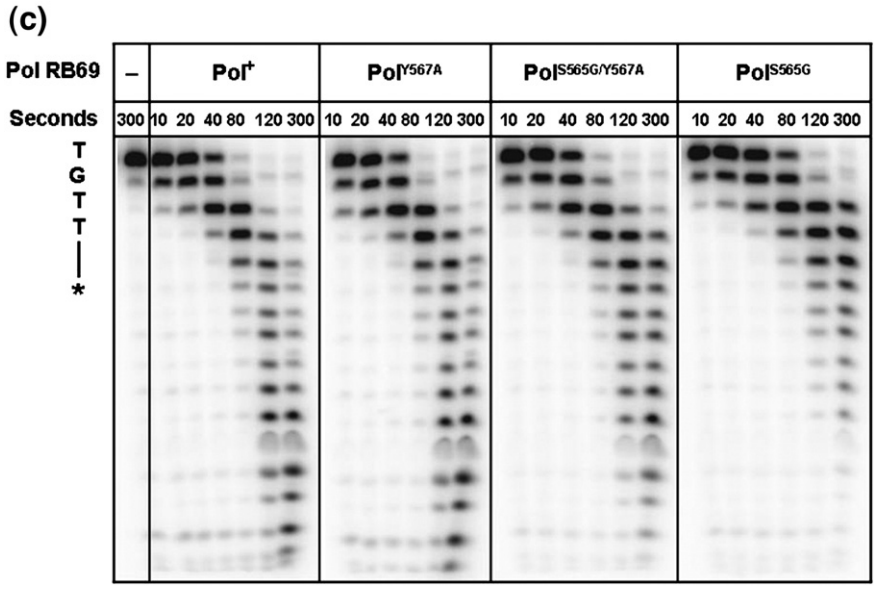

Fig. 3 (*continued*)

lethally mutated progeny phage. In the complementation assay, the $Pol^{S565G/Y567A}$ Exo^- polymerase is also unable to support the growth of T4 *43amam* but can support the growth of T4 43^+ (Fig. 8), suggesting that Pol^+ can compete sufficiently with $Pol^{S565G/Y567A}$ to produce some viable progeny whose plaques are, however, small compared to T4 plaques growing on BB cells harboring a plasmid expressing Pol^+ Exo^- or Pol^{S565G} Exo^-.

Discussion

Reversal of a powerful mutator activity by a nearby fidelity-neutral substitution

The phage RB69 DNA polymerase mutant Pol^{Y567A} displays a powerful mutator activity that can exceed 10^3-fold at some sites.[1,16] In the crystal structure of the RB69 DNA polymerase ternary complex, Y567 displays an unfavorable rotamer conformation that is maintained by hydrogen-bonding interactions with two nearby residues.[20] These interactions are essential for forming a nucleotide binding pocket. The aromatic phenyl ring of Y567 plays an important role in base discrimination, forming a hydrogen bond with the minor-groove edge of the DNA duplex at the primer terminus and thus helping to check Watson–Crick base-pair geometry. Removing the γ-hydroxyl from Y567 (Y567F) disrupts the hydrogen-bonding network, allows Y567F to adopt a more favorable rotamer conformation that distorts the nucleotide binding pocket, reduces the affinity of incoming dNTP, and blocks DNA replication.[20] On the other hand, replacing the phenolic side chain with a methyl group (Y567A) produces a vigorous polymerase that is a powerful base substitution mutator both *in vivo* and *in vitro* and a moderate mutator for frameshift mutations *in vitro*. The Pol^{Y567A} mutant polymerase is better able to accommodate noncanonical base-pairings, and the Y→A replacement does not interfere with the geometry of correctly paired bases.[1,16] Thus, Y567 plays a major role in base discrimination by providing a steric gate to check pairing (Fig. 9).

The role of Ser565 in maintaining fidelity has come under scrutiny only recently. Because Ser565 contributes to the rear wall of the binding pocket, we expected the S565G replacement to enlarge the size of the pocket, thus more readily accepting base mispairs and displaying mutator activity. However, the Pol^{S565G} polymerase displays, at most, very weak mutator and antimutator activities both *in vivo* and *in vitro* (Tables 1–5). We also anticipated that the double mutant $Pol^{S565G/Y567A}$ polymerase would contain a further expanded nucleotide binding pocket compared with the Pol^{Y567A} polymerase and would therefore display further increased mutation rates. Surprisingly, however, the $Pol^{S565G/Y567A}$ polymerase displayed sharply *decreased* mutation rates both *in vivo* and *in vitro* compared to the Pol^{Y567A} polymerase (Tables 1–5). On average, $Pol^{S565G/Y567A}$ was 50-fold more accurate than Pol^{Y567A} in *rII* reversion assay and 40-fold more accurate in *rI* forward mutation assay.

L561 is another residue that contributes to the geometry of the Pol pocket and, when reduced in bulk by the L561A replacement, displays modest mutator activities in mutation tests *in vivo* and in kinetic assays *in vitro*.[10] In contrast to the antimutagenic action of S565G in the $Pol^{S565G/Y567A}$ context, we observed no antimutagenic effect of L561A in the $Pol^{L561A/S565G}$ context (data not shown). Combining the L561A and Y567A replacements produced a

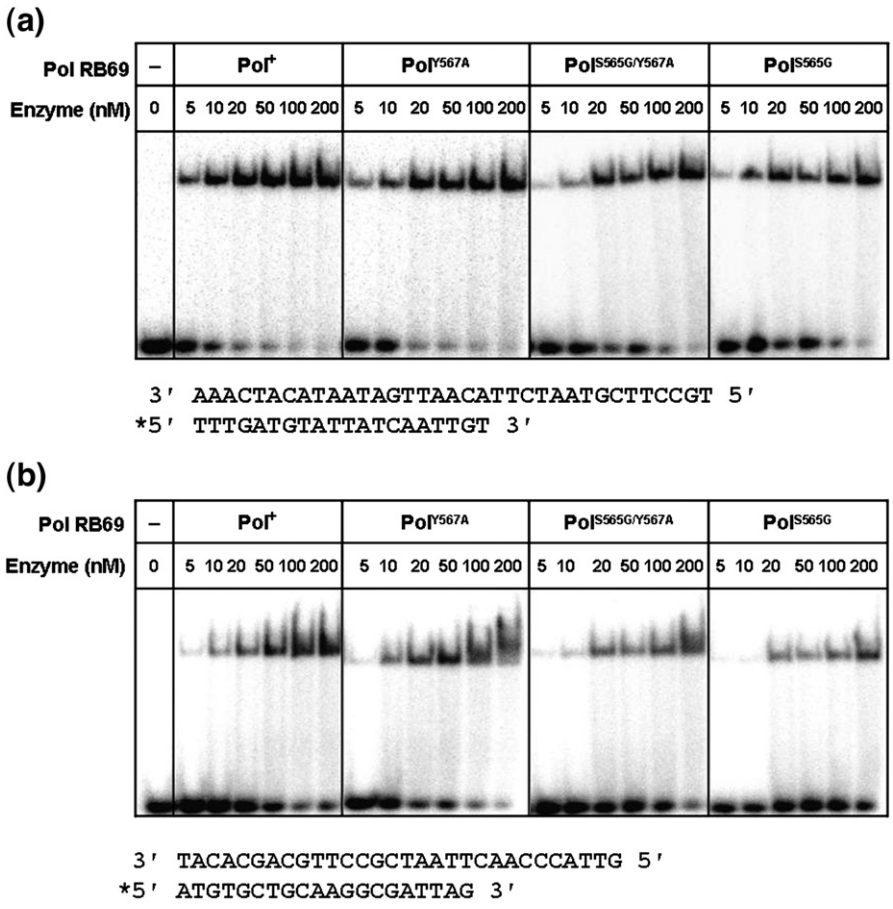

Fig. 4. RB69 DNA polymerase binding to dsDNA with normal base-pairing or a terminal G·T mismatch. The 5′-labeled double-stranded substrates (5 nM) were incubated with indicated RB69 polymerases at 5 nM, 10 nM, 25 nM, 50 nM, 100 nM, and 200 nM. After gel electrophoresis, the bands corresponding to bound or free DNA were quantified by autoradiography. (a) Binding to normal dsDNA. (b) Binding to mismatched dsDNA.

polymerase with exceptionally high mutation rates, and the strong mutator phenotype was again suppressed when S565G was added to the combination (data not shown).

Associated biochemical parameters

We searched for altered behaviors that might explain the sharply contrasting fidelities of the Pol$^{S565G/Y567A}$ and Pol^{Y567A} polymerases. Polymerase activities were modestly reduced both *in vitro* and *in vivo*, but not in informative ways. Proofreading estimated by comparing mutation rates in the Exo$^+$ and Exo$^-$ versions of the mutant polymerases (Table 4), and exonuclease activities on either dsDNA or ssDNA (Fig. 3) were uninformative as to the fidelity paradox. In mispair formation and extension assays *in vitro* under both standing-start and running-start conditions, the Pol$^+$, Pol^{S565G}, and Pol$^{S565G/Y567A}$ polymerases were inefficient, while the Pol^{Y567A} polymerase was substantially more efficient—results consistent with, but not explaining, the mutation patterns. Pre-steady-state kinetic data showed that the Pol$^+$, Pol^{S565G}, and Pol$^{S565G/Y567A}$ polymerases display high $K_{d,app}$ values for both G·dTMP and T·dGMP mispairs, while the Pol^{Y567A} polymerase has reduced $K_{d,app}$ values for both mispairs.[22] Our present kinetic data for the Pol$^+$ and Pol^{Y567A} polymerases are in good agreement with published data.

Table 6. DNA binding affinities of Exo$^+$ RB69 DNA polymerase mutants

Polymerase	$K_{d(DNA)}$ (nM) [dsDNA]	$K_{d(DNA)}$ (nM) [dsDNA, T·G mismatch]
Pol$^+$	6.9 ± 2.1	38.2 ± 4.3
Pol^{Y567A}	13.2 ± 1.4	25.7 ± 3.2
Pol^{S565G}	38.9 ± 3.4	132.1 ± 5.7
Pol$^{S565G/Y567A}$	29.9 ± 1.9	79.9 ± 4.8

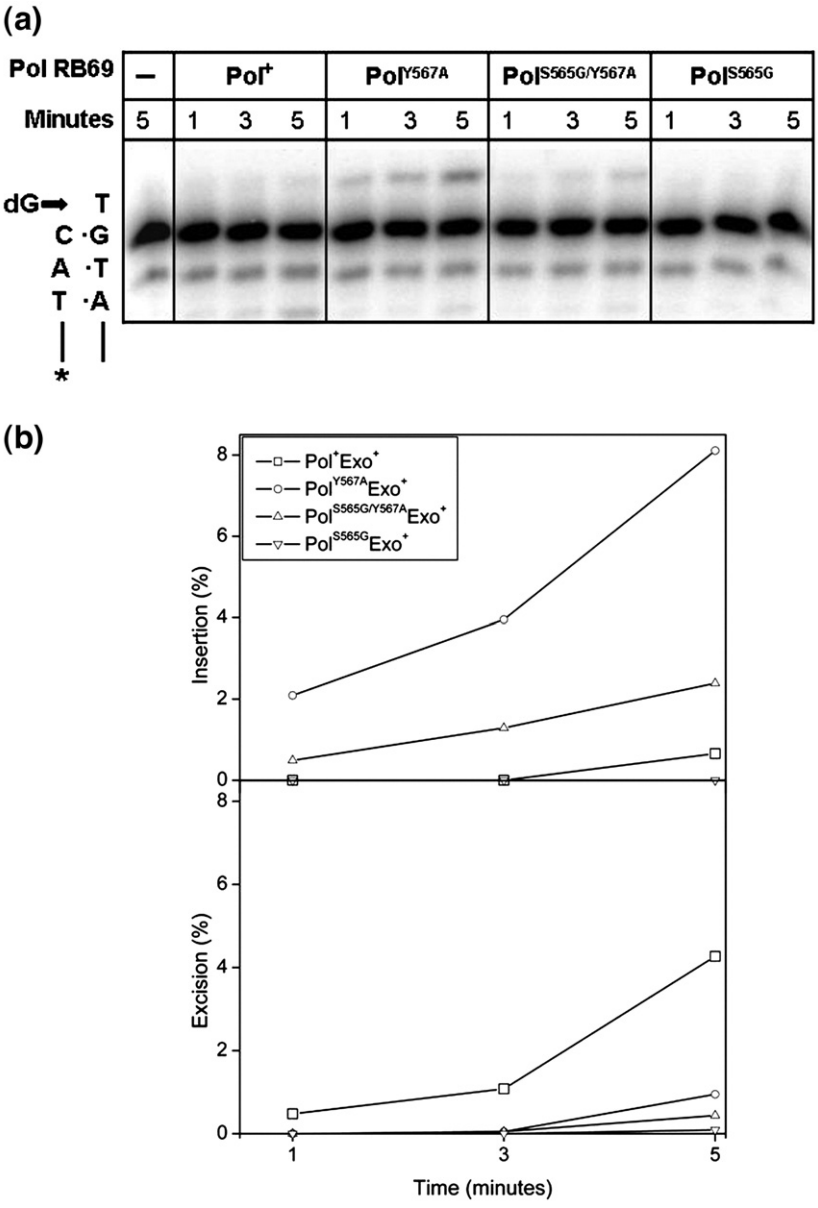

Fig. 5. T·dGTP mismatch formation by RB69 DNA polymerases. (a) A ^{32}P-labeled primer/template was present at 50 nM in all reactions. The sequence of a portion of the substrate is shown on the left with an incoming dGTP ("dG"). For each polymerase, 0.05 nM enzyme and 1 mM dGTP were incubated for 1 min, 3 min, and 5 min. A band at the +1 position indicates insertion of dGMP, while bands below the primer are degradation products. (b) Percentages of mismatch insertion and primer degradation are plotted against reaction time for each of the polymerases.

An article (M. Wang, *et al*., unpublished results) explores the kinetic parameters of mispair formation, extension, and proofreading using templates that mimic the sequences of either a mutational hot spot or a region of apparently low mutation rates in the rI mutation reporter used here. Although not addressing the question on the antimutagenic properties of the S565G replacement, the assays do largely reproduce *in vitro* the relative mutation rates observed by us *in vivo* as a function of local sequence, the first such demonstration known to us. Because spontaneous mutation rates vary greatly from site to site (for instance, by about 10^3-fold in phage T4[23]), *rII* reversion rates are expected to vary considerably among sites, and mutation spectra typically show a wide range of site-specific rates of forward mutation. Thus, it is often desirable to use a diversity of substrates for kinetics studies of polymerase accuracy.

Based on measurements of DNA binding using gel retardation assays with correct or mispaired termini, the Pol^{S565G} and Pol$^{S565G/Y567A}$ polymerases displayed weaker binding compared to the Pol$^+$ or Pol^{Y567A} polymerases (Fig. 4 and Table 6). Weaker DNA binding for both Pol^{S565G} and Pol$^{S565G/Y567A}$ polymerases compared to Pol$^+$ and Pol^{Y567A} polymerases may reflect less specific polymerase–DNA interactions whose *in vivo* consequences could be manifested in a less efficient DNA synthesis, but direct extrapolation to replication *in vivo* is difficult and requires caution. Using a

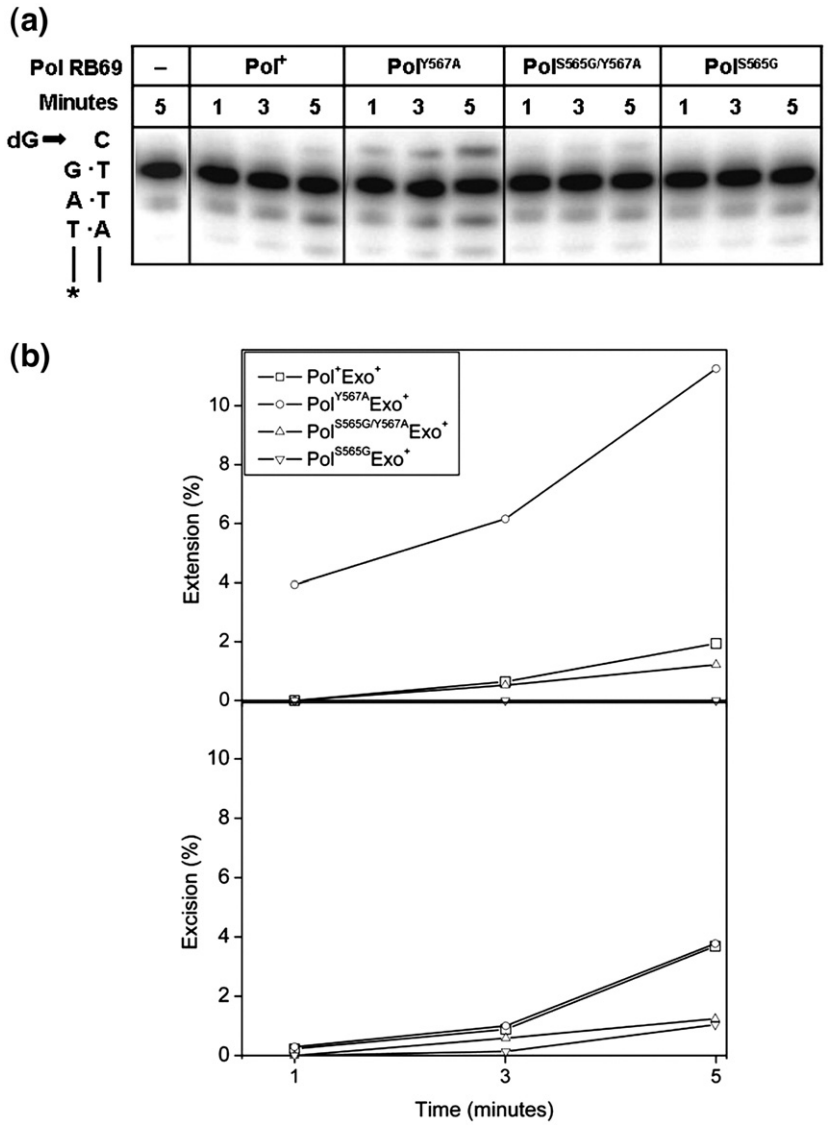

Fig. 6. T-dGMP mismatch extension by RB69 DNA polymerases. (a) A ^{32}P-labeled primer/template with a terminal T-dGMP mismatch was present at 50 nM in all reactions. The sequence of a portion of the substrate is shown on the left. For each polymerase, 0.05 nM enzyme and 1 mM correct dGTP were incubated for 1 min, 3 min, and 5 min. (b) Percentages of mismatch extension and primer degradation are plotted *versus* reaction time for each of the polymerases.

different assay and different interaction conditions, no such difference were observed (M. Wang, *et al.*, unpublished results).

Candidate mechanisms for the antimutagenic activity of S565G

One possible explanation for the increased fidelity of the Pol$^{S565G/Y567A}$ polymerase compared to Pol^{Y567A} is the increased partitioning of the mismatched primer-terminus to the Exo site. Diverse changes in the Pol site can perturb the tight coordination between the Pol cycle and the Exo cycle,[6,24] and changing Y567 to alanine not only enlarges the nucleotide binding pocket but probably affects Pol/Exo partitioning in favor of the Pol site,[1,16] increasing mismatch extension and thus decreasing proofreading. Conversely, proofreading may become more proficient with any inhibition in polymerization, as might be caused by mutations in the Pol site that reduce the ability to form polymerizing complexes and thus shift the balance in favor of Exo complexes.[14,15] (A side effect is that increased proofreading lowers discrimination between mismatched primer termini and matched primer-termini and increases the degradation of newly synthesized DNA.[25,26]) Because both Pol^{Y567A} and Pol$^{S565G/Y567A}$ enzymes bind less tightly to dsDNA substrates (Fig. 4 and Table 6), they are expected to form exonuclease complexes more readily and, as a consequence, to display increased exonuclease activities. However, we observed no such increase in exonuclease activity. One explanation for this failure would be increased polymerase dissociation from the primer/template DNA (whether or not mismatched), followed by rebinding to DNA to form either an Exo complex in

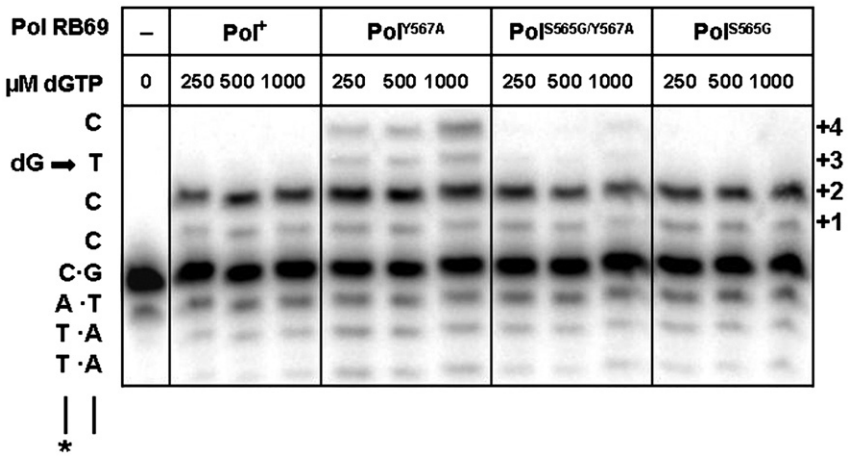

Fig. 7. Running-start reactions for T·dG mismatch formation and extension for the indicated RB69 DNA Exo$^+$ polymerases. A ^{32}P-labeled primer/template was present at 50 nM in all reactions. A partial sequence of the substrate is shown on the left. The reaction conditions were the same as for the standing-start reactions, and the reaction time was 5 min. dGTP was added at the indicated concentrations (μM). RB69 Pol^{Y567A} not only inserts dGTP opposite template T (band +3) but extends the mismatch, creating the next correct G·C base pair (band +4). Neither the Pol$^+$ enzymes nor the Pol^{S565G} enzymes can create the mismatch, but terminate synthesis at band +2. The Pol$^{S565G/Y567A}$ double mutant has a sharply reduced ability to insert, extend, and create a second mismatch compared to Pol^{Y567A}.

the presence of a mismatch or a Pol complex and continued replication. T4 DNA polymerase molecules do exchange during DNA replication,[27] and RB69 would be expected to do the same. Frequent dissociation will increase the opportunity to excise a mismatch by either the original polymerase molecule or another polymerase molecule, and thus may be responsible for the increased fidelity of replication by Pol$^{S565G/Y567A}$ compared to Pol^{Y567A}. This explanation for the increased fidelity of Pol$^{S565G/Y567A}$ compared to Pol^{Y567A} is supported by our observation of decreased DNA binding by the Pol^{Y567A} and Pol$^{S565G/Y567A}$ enzymes, but is challenged by the failure to observe such a difference (M. Wang, *et al.*, unpublished results). However, the conditions used

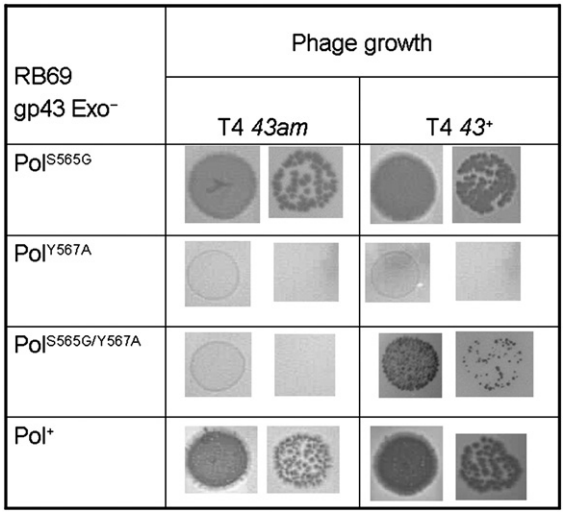

Fig. 8. Complementation assay. Phage growth images are spot tests in which 20,000 (left) or 100 (right) viable particles of either T4 *43am* or *43*$^+$ were spotted onto lawns of cells carrying a plasmid producing the indicated Exo$^-$ RB69 gp43.

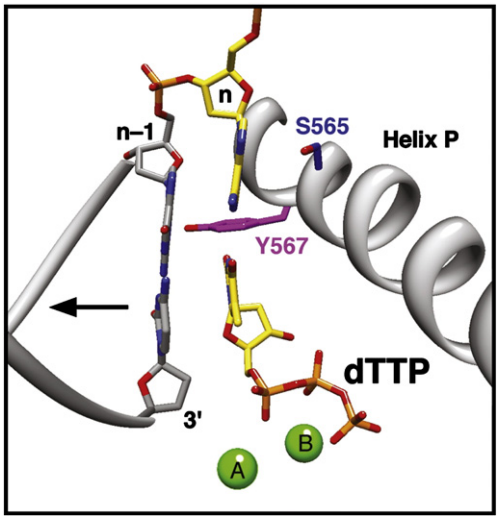

Fig. 9. A view of the major groove edge of the nascent dTTP·dA base-pair binding pocket illustrating the positions of Ser565 and Tyr567 in α-helix P (wide gray ribbon). "*n*" indicates the template dA, and "*n*−1" indicates the nucleotide upstream of the templating nucleotide. The active-site metals are represented as green spheres A and B. The arrow indicates the upstream direction of the DNA duplex. The narrow gray ribbon represents the duplex DNA backbone (residues omitted for clarity). The image was created in Chimera[21] from Protein Data Bank ID 1IG9.

in the two measurements were different, so that decreased binding remains a possibility *in vivo*.

Note also that a more frequent dissociation from the primer/template would also tend to result in the production of large deletions, as observed *in vitro* in the absence of the gp45 processivity clamp (Table 5). The inhibition of a large deletion mutagenesis between direct repeats by accessory proteins *in vitro* was observed previously for RB69 DNA polymerase and yeast DNA polymerase δ.[16,28]

Another explanation for the increased fidelity of the $Pol^{S565G/Y567A}$ polymerase compared to Pol^{Y567A} is provided by the wealth of crystallographic data (M. Wang, *et al*., unpublished results). One key observation is that the replacement of the bulky Y567 side chain by alanine reduces the rigidity of the Pol pocket in the Y567A single mutant by disrupting the hydrogen-bonding network involving the OH groups of Y567, Y391, and T587, so that the templating base can be displaced downward to accommodate mispairs. When the S565G replacement was introduced into the Y567A mutant, base selectivity was increased compared to Pol^{Y567A} even though the volume of the Pol pocket was somewhat greater in the $Pol^{Y567A/S565}$ double mutant than in Pol^{Y567A}. This appeared to be due to an increase in the hydrophobic van der Waals interactions of G565 with the templating base, making it more rigid.

The two candidate explanations for the antimutagenic impact of S565G on Y567A are not mutually exclusive.

Materials and Methods

Construction, expression, and purification of RB69 DNA polymerase variants

Plasmids pCW19R and pCW.50R were generous gifts from Jim Karam (Tulane University). Plasmid pCW19R carries a wild-type RB69 gene *43* (encoding the gp43 polymerase) under the control of the T7 Φ10 promoter of the cloning vector pSP72 (Promega). Plasmid pCW.50R encodes a Pol^{+} Exo^{-} polymerase carrying the exonuclease-inactivating replacements D222A and D327A. Site-directed mutagenesis to create the Pol^{S565G}, Pol^{Y567A}, and $Pol^{S565G/Y567A}$ variants was carried out using the Stratagene QuikChange Site-Directed Mutagenesis protocol and was confirmed by sequencing. Expression and purification of the Pol^{S565G}, Pol^{Y567A}, and $Pol^{S565G/Y567A}$ gp43 s were performed as previously described.[17]

Mutation tests *in vivo*

Reversion tests using T4 *rII* mutations were performed as described previously.[1] T4 *43amam rII* mutants were used to infect *E. coli* BB cells carrying a plasmid expressing the desired allele of RB69 gene *43*. *rII131* reverts by +1 (A5→A6), *rIIUV232* reverts by −1 (A3→A2), *rIIUV256* reverts by G·C→A·T transitions, and *rIIUV375* reverts probably by both transitions and transversions at three adjacent A·T sites. Forward mutation *rI* assays were also performed as described previously.[1] To determine the kinds of *rI* mutations introduced *in vivo* by various RB69 polymerase mutants, we collected mutants of independent origin, we resuspended mutant plaques in 40 μl of water, and we amplified the *rI* gene by PCR and sequenced it as described previously.[1] When sequencing was not performed, a historical correction factor of 0.64 was used to estimate the frequencies of *rI* mutants among all *r* mutants.

Mutation tests *in vitro*

Mutation tests *in vitro* were performed with phage M13mp2 *lacZ*α-gapped substrates prepared as described previously.[19] The incubation mixture (25 μl) contained 25 mM Tris-acetate (pH 7.5), 10 mM Mg-acetate, 150 mM K-acetate, 2 mM dithiothreitol, 150 ng of M13mp2 *lacZ*α-gapped substrate, 1 mM of each dNTP, and 7–10 pmol of wild-type or mutant polymerase. Reactions were incubated at 37 °C for 30 min, stopped by addition of ethylenediaminetetraacetic acid, and analyzed by agarose gel electrophoresis. Products of reactions in which gap filling was complete were introduced into MC1061 cells and plated on CSH50 cells to score M13 plaques as either wild-type (dark blue) or mutant (white to less dark blue). A representative set of mutants from most collections was sequenced to determine the types of errors and to adjust the mutation frequency for rare phenotypic mutants without a mutation in the *lacZ*α reporter and for mutants with more than one detectable mutation; a historical correction factor of 0.95 was applied to mutant frequencies when sequencing was not performed. Mutation rates (μ) were calculated as described previously[19] by multiplying the net mutant frequency [adjusted for the historical background (6.2×10^{-4}) of uncopied *lacZ*α DNA] by the proportion of mutants in each class and dividing by 0.6 (a correction factor for detecting errors in *E. coli*) and by the number of detectable sites (opportunities) for each class of mutation.

DNA synthesis *in vivo*

T4 *43amam* was used to infect *E. coli* BB cells carrying a plasmid expressing the desired allele of RB69 gene *43*. At 22 min after infection, 20μCi/ml [^{3}H]thymidine was added (at a specific activity of 20 μCi/μg dT). After 15 min, ^{3}H labeling was terminated in an ice bath, and trichloroacetic-acid-precipitable ^{3}H counts were determined. Measurements of DNA synthesis *in vivo* were performed as previously described.[1]

Polymerase-specific activity

Polymerase-specific activity was measured by the incorporation of [α-^{32}P]dATP (Hartmann Analytic) into activated calf thymus DNA (Sigma), as previously described.[8]

DNA substrates

All nucleotides were purchased from the Laboratory of DNA Sequencing and Oligonucleotide Synthesis (Institute

of Biochemistry and Biophysics, Warsaw) and purified on a 20% polyacrylamide gel with 7 M urea. All primers were 5′ end labeled with [γ-^{32}P]dATP (5000 Ci/mmol; Hartmann Analytic) using T4 DNA polynucleotide kinase (Takara). Annealing of primer to template was performed in 10 mM Tris–HCl (pH 7.5) at a primer/template molar ratio of 1:1.3. The primer/template was annealed at 75 °C for 5 min and allowed to cool slowly to 25 °C.

DNA gel retardation assay

The interactions of RB69 wild-type or mutant gp43 s with dsDNA were assayed using 5′-end-labeled 20-mer (5′-TTTGATGTATTATCAATTGT-3′) hybridized to a 1.3 molar excess of complementary 35-mer (5′-TGCCTTCGTAATCTTACAATTGATAATACATCAAA-3′). The interactions of RB69 polymerases with a mispaired primer terminus were assayed using a 5′-end-labeled 20-mer (5′-ATGTGCTGCAAGGCGATTAG-3′) hybridized to a 30-mer (5′-GTTACCCAACTTAATCGCCTTGCAGCA-CAT-3′). The 10-μl reaction mixture contained 10 mM Hepes (pH 8.0), 0.5 mM dithiothreitol, 1 μg of bovine serum albumin, 10 mM ethylenediaminetetraacetic acid (EDTA), 5 nM DNA substrate, and increasing concentrations of gp43. After incubation for 5 min at 4° C, products were separated on a precooled 6% polyacrylamide nondenaturing gel and quantitated on a Fuji PhosphorImager. To determine $K_{d(DNA)}$, we plotted the reciprocal of the fraction of DNA shifted as a function of enzyme concentration.

Exonuclease activity

Assays of dsDNA and ssDNA 3′→5′ exonuclease activities were performed as previously described.[17] Exo activity on mismatched DNA was assayed under the same conditions using 5 nM gp43 and 50 nM ^{32}P 5′-end-labeled 20-mer (5′-ATGTGCTGCAAGGCGATTAG-3′) annealed to 30-mer (5′-GTTACCCAACTTAATCGCCTTGCAGCA-CAT-3′).

Extension of a primer-terminus mismatch

The assay for the extension of a terminal T·dGMP mismatch contained 50 nM ^{32}P 5′-end-labeled 20-mer (5′-ATGTGCTGCAAGGCGATTAG-3′) annealed to 30-mer (5′-GTTACCCAACTTAATCGCCTTGCAGCACAT-3′). The 10-μl reaction mixture contained 25 mM Tris-acetate (pH 7.5), 10 mM Mg-acetate, 2 mM DTT, 0.05 nM gp43, and 1 mM dGTP. Reactions were incubated at 37 °C for 1 min, 3 min, and 5 min, and then quenched by addition of stop-dye solution. Product bands were resolved by electrophoresis on a 16% polyacrylamide gel with 7 M urea, analyzed by autoradiography, and quantified by densitometry.

Misinsertion assay

The substrate for the misinsertion of dGMP opposite template T under standing-start conditions was ^{32}P 5′-end-labeled 20-mer (5′-ATGTGCTGCAAGGCGATTAC-3′) annealed to a complementary 27-mer (5′-GTAAGATG-TAATCGCCTTGCAGCACAT-3′). The reaction mixture contained 25 mM Tris-acetate (pH 7.5), 10 mM Mg-acetate, 2 mM DTT, 50 nM DNA substrate, 0.05 nM gp43, and 1 mM dGTP. Reactions were incubated at 37 °C for 1 min, 3 min, and 5 min, and then quenched by addition of stop-dye solution.

Running-start assays were conduced in the same reaction buffer. The 10-μl reaction mixture contained 50 nM ^{32}P 5′-end-labeled 20-mer (5′-ATGTGCTG-CAAGGCGATTAC-3′) annealed to a complementary 27-mer (5′-GAACTCCGTAATCGCCTTGCAGCACAT-3′), 0.05 nM gp43, and increasing concentrations of dGTP (250 μM, 500 μM, and 1000 μM). Reactions were incubated at 37 °C for 5 min and quenched by the addition of 5 μl of stop-dye solution. Product bands were resolved by electrophoresis on a 16% polyacrylamide gel with 7 M urea, analyzed by autoradiography, and quantified by densitometry.

Acknowledgements

We thank Bill Beard for providing Fig. 9 and both Bill Beard and Mike Murray for critical readings of the manuscript and Bill Konigsberg for advice on the implications of his structural models. This research was supported, in part, by funds allocated to project number Z01ES061054 of the Intramural Research Program of the National Institutes of Health, National Institute of Environmental Health Sciences, USA, and by grant N301014433 from the Polish Ministry of Science and Higher Education (to A.B.).

References

1. Bebenek, A., Dressman, H. K., Carver, G. T., Ng, S., Petrov, V., Yang, G. *et al.* (2001). Interacting fidelity defects in the replicative DNA polymerase of bacteriophage RB69. *J. Biol. Chem.* **276**, 10387–10397.
2. Wang, J., Sattar, A. K., Wang, C. C., Karam, J. D., Konigsberg, W. H. & Steitz, T. A. (1997). Crystal structure of a pol alpha family replication DNA polymerase from bacteriophage RB69. *Cell*, **89**, 1087–1099.
3. Shamoo, Y. & Steitz, T. A. (1999). Building a replisome from interacting pieces: sliding clamp complexed to a peptide from DNA polymerase and a polymerase editing complex. *Cell*, **99**, 155–166.
4. Franklin, M. C., Wang, J. & Steitz, T. A. (2001). Structure of the replicating complex of a pol alpha family DNA polymerase. *Cell*, **105**, 657–667.
5. Li, Y., Korolev, S. & Waksman, G. (1998). Crystal structures of open and closed forms of binary and ternary complexes of the large fragment of *Thermus aquaticus* DNA polymerase I: structural basis for nucleotide incorporation. *EMBO J.* **17**, 7514–7525.
6. Kunkel, T. A. & Bebenek, K. (2000). DNA replication fidelity. *Annu. Rev. Biochem.* **69**, 497–529.

7. Kunkel, T. A. (2004). DNA replication fidelity. *J. Biol. Chem.* **279**, 16895–16898.
8. Zhong, X., Pedersen, L. C. & Kunkel, T. A. (2008). Characterization of a replicative DNA polymerase mutant with reduced fidelity and increased translesion synthesis capacity. *Nucleic Acids Res.* **36**, 3892–3904.
9. Yang, G., Franklin, M., Li, J., Lin, T. C. & Konigsberg, W. (2002). A conserved Tyr residue is required for sugar selectivity in a Pol alpha DNA polymerase. *Biochemistry*, **41**, 10256–10261.
10. Zhang, H., Rhee, C., Bebenek, A., Drake, J. W., Wang, J. & Konigsberg, W. (2006). The L561A substitution in the nascent base-pair binding pocket of RB69 DNA polymerase reduces base discrimination. *Biochemistry*, **45**, 2211–2220.
11. Echols, H. & Goodman, M. F. (1991). Fidelity mechanisms in DNA replication. *Annu. Rev. Biochem.* **60**, 477–511.
12. Goodman, M. F., Creighton, S., Bloom, L. B. & Petruska, J. (1993). Biochemical basis of DNA replication fidelity. *Crit. Rev. Biochem. Mol. Biol.* **28**, 83–126.
13. Fidalgo da Silva, E., Mandal, S. S. & Reha-Krantz, L. J. (2002). Using 2-aminopurine fluorescence to measure incorporation of incorrect nucleotides by wild type and mutant bacteriophage T4 DNA polymerases. *J. Biol. Chem.* **277**, 40640–40649.
14. Spacciapoli, P. & Nossal, N. G. (1994). A single mutation in bacteriophage T4 DNA polymerase (A737V, tsL141) decreases its processivity as a polymerase and increases its processivity as a 3′→5′ exonuclease. *J. Biol. Chem.* **269**, 438–446.
15. Reha-Krantz, L. J. (2010). DNA polymerase proofreading: multiple roles maintain genome stability. *Biochim. Biophys. Acta*, **1804**, 1049–1063.
16. Bebenek, A., Carver, G. T., Dressman, H. K., Kadyrov, F. A., Haseman, J. K., Petrov, V. *et al.* (2002). Dissecting the fidelity of bacteriophage RB69 DNA polymerase: site-specific modulation of fidelity by polymerase accessory proteins. *Genetics*, **162**, 1003–1018.
17. Jacewicz, A., Makiela, K., Kierzek, A., Drake, J. W. & Bebenek, A. (2007). The roles of Tyr391 and Tyr619 in RB69 DNA polymerase replication fidelity. *J. Mol. Biol.* **368**, 18–29.
18. Schultz, G. E., Jr, Carver, G. T. & Drake, J. W. (2006). A role for replication repair in the genesis of templated mutations. *J. Mol. Biol.* **358**, 963–973.
19. Bebenek, K. & Kunkel, T. A. (1995). Analyzing fidelity of DNA polymerases. *Methods Enzymol.* **262**, 217–232.
20. Yang, G., Wang, J. & Konigsberg, W. (2005). Base selectivity is impaired by mutants that perturb hydrogen bonding networks in the RB69 DNA polymerase active site. *Biochemistry*, **44**, 3338–3346.
21. Pettersen, E. F., Goddard, T. D., Huang, C. C., Couch, G. S., Greenblatt, D. M., Meng, E. C. & Ferrin, T. E. (2004). UCSF Chimera—a visualization system for exploratory research and analysis. *J. Comput. Chem.* **25**, 1605–1612.
22. Zhang, H., Beckman, J., Wang, J. & Konigsberg, W. (2009). RB69 DNA polymerase mutants with expanded nascent base-pair-binding pockets are highly efficient but have reduced base selectivity. *Biochemistry*, **48**, 6940–6950.
23. Ronen, A. & Rahat, A. (1976). Mutagen specificity and position effects on mutation in T4rII nonsense sites. *Mutat. Res.* **34**, 21–34.
24. Muzyczka, N., Poland, R. L. & Bessman, M. J. (1972). Studies on the biochemical basis of spontaneous mutation: I. A comparison of the deoxyribonucleic acid polymerases of mutator, antimutator, and wild type strains of bacteriophage T4. *J. Biol. Chem.* **247**, 7116–7122.
25. Clayton, L. K., Goodman, M. F., Branscomb, E. W. & Galas, D. J. (1979). Error induction and correction by mutant and wild type T4 DNA polymerases. Kinetic error discrimination mechanisms. *J. Biol. Chem.* **254**, 1902–1912.
26. Gauss, P., Doherty, D. H. & Gold, L. (1983). Bacterial and phage mutations that reveal helix-unwinding activities required for bacteriophage T4 DNA replication. *Proc. Natl Acad. Sci. USA*, **80**, 1669–1673.
27. Yang, J., Zhuang, Z., Roccasecca, R. M., Trakselis, M. A. & Benkovic, S. J. (2004). The dynamic processivity of the T4 DNA polymerase during replication. *Proc. Natl Acad. Sci. USA*, **101**, 8289–8294.
28. Fortune, J. M., Stith, C. M., Kissling, G. E., Burgers, P. M. & Kunkel, T. A. (2006). RPA and PCNA suppress formation of large deletion errors by yeast DNA polymerase delta. *Nucleic Acids Res.* **34**, 4335–4341.